Nuclear Materials and Energy 000 (2017) 1–6

Contents lists available at ScienceDirect

Nuclear Materials and Energy

journal homepage: www.elsevier.com/locate/nme

Heat flux measurements and modelling in the RFX-mod experiment

P. Innocente[a,*], H. Bufferand[b], A. Canton[a], G. Ciraolo[b], N. Visonà[a,c]

[a] Consorzio RFX (CNR, ENEA, INFN, Università di Padova, Acciaierie Venete SpA), Corso Stati Uniti 4 - 35127 Padova, Italy
[b] CEA, IRFM, 13108 St Paul-Lez-Durance, France
[c] Università degli studi di Padova, Padova, Italy

ARTICLE INFO

Article history:
Received 12 July 2016
Revised 15 December 2016
Accepted 18 January 2017
Available online xxx

ABSTRACT

The knowledge of edge plasma transport parameters and plasma edge phenomena is a key element in the design of the first wall for a magnetically confined fusion experiment. In RFX-mod heat flux measurement and edge transport modelling have been done to improve the understanding of this aspect. Heat flux deposition profiles have been evaluated from infrared temperature measurements of insertable graphite limiters. They were inserted up to 12 mm into the reversed field pinch plasma of ohmically heated discharges with $I_p = 0.6 \div 1.0$ MA, $n_e = 0.5 \div 3 \cdot 10^{19}$ m^{-3} ($n/n_G < 0.7$) and total power of about 10÷15 MW. Strong asymmetries in heat flux deposition have been measured in poloidal direction at low density between the electron and the ion drift side and smaller ones in toroidal direction when $q(a) \neq 0$. The poloidal asymmetry has been associated to the presence of superthermal electrons [1] while the toroidal one has been less clearly identified as due to the small toroidal extension of the limiters. To account for the 2D deposition nature of heat load on the surface of the employed limiters, a simple 3D code has been developed to evaluate heat flux from temperature data. In this way at the deeper limiter insertions a heat flux decay length of about 2 mm and 2.5 mm has been evaluated in electron and ion drift sides. Modelling of the evaluated heat fluxes has been done using the SOLEDGE2D-EIRENE edge code [2]. This fluid code is well suited for the RFX-mod wall limiter configuration because, thanks to the implemented penalization technique, the computational domain can be extended up to the entire first wall. Edge modelling has shown that measured decay lengths are compatible with energy diffusion coefficients in Scrape Off Layer (SOL) smaller than those commonly evaluated at plasma edge; the cause of the reduced diffusion in the SOL will be discussed in the paper.

1. Introduction

The study of transport phenomena and the evaluation of transport parameters at the plasma Edge/SOL is a key element for the improvement of plasma performance and the optimization of the first wall (FW) response to the plasma wall interaction (PWI). In the Reversed Field Pinch (RFP) devices these phenomena have not been investigated thoroughly mainly because most of the resources were devoted to the reduction of the core transport due to the magnetic stochasticity; but also because the presence of strong deformation of the last close flux surface (LCFS) and edge $m = 0$ magnetic islands makes measurements and fluid description of the transport rather difficult. In the RFX-mod device ($R/a = 2/0.46$ m, $I_t \leq 2$ MA) [3,4] these problems of the RFP configuration have been partially reduced in the last years thanks to the achievement of the Quasi Single Helicity (QSH) states, which are characterized by an improved core confinement [5] and by better control of LCFS deformation by feedback control of edge radial fields [4,6]. Furthermore in RFX-mod case the knowledge of the transport parameters at the plasma edge is a necessary element for the design of the foreseen device upgrade in which plasma boundary will play a fundamental role [6].

In this paper we present the first attempt to study the transport in the plasma Edge/SOL of the RFX-mod device analysing the power load on an insertable graphite limiter and modelling it with a 2D edge fluid code. To evaluate the power we have measured the temperature evolution of the limiter surface with an infrared camera. To extract quantitative information on plasma transport from the computed heat flux we have used the SOLEDGE2D-EIRENE edge fluid code [2].

In the next sections we will describe the experimental setup first, briefly the method to compute the heat flux from the tem-

* Corresponding author. Corso Stati Uniti, 5, 35127, Padova, Italy.
E-mail address: paolo.innocente@igi.cnr.it (P. Innocente).

http://dx.doi.org/10.1016/j.nme.2017.01.020

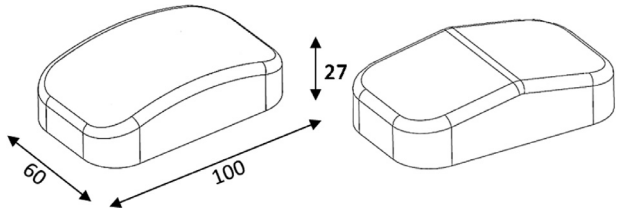

Fig. 1. Drawing of the cylindrical and flat sloped limiters.

perature measurement, then we will analyse the measurements in terms of global plasma parameters and finally we present the results of the edge modelling.

2. Experimental setup

To measure the heat flux two different limiters have been used, one with a cylindrical surface and one with two flat sloped surfaces (Fig. 1). Limiters have been prepared in two grades of polycrystalline graphite: the same one used for the RFX-mod wall tiles with a thermal conductivity ≈100 W/m·K (MERSEN, type 5890PT) and a second one with an improved thermal conductivity of ≈150 W/m·K (Toyo Tanso, type IG15). Most of the measurements have been performed using the cylindrical shaped limiter made with the 5890PT graphite. The cylindrical shape slightly complicates the evaluation of the parallel heat flux but has the advantage of reducing the achieved maximum temperature. The temperature of the limiter surface has been measured by an infrared camera (Flir A655sc [7]), with a time resolution of 5 ms operating in the 7.5÷14 µm infrared range, installed at the same poloidal section of the limiter (Fig. 2). The relatively low time resolution of the camera prevents a detailed correlation with some fast phenomena present in the RFX-mod discharges; compared to faster MIR cameras, this disadvantage is compensated by the negligible noise due to molecular emission, which severely affected our previous attempt to measure surface temperature in NIR/MIR range and also by the lower error in case of dust [8]. The principal drawback of the experimental setup was the small toroidal extension of the limiter: the vertical port aperture constrained the toroidal width to 60 mm only. With such dimension, the material object acts as a true limiter only when the toroidal field is nearly zero at the limiter radius, a condition that translates to an upper limit on the safety factor $|q(a)| \leq 0.002$. This condition is met in stationary operations, because in RFX-mod the improved QSH state corresponds to the lowest values of |q(a)|, but not during the fast dynamo relaxation events, during which q(a) becomes more negative and the object collects the parallel heat flux from distances much longer than half poloidal turn.

The limiter has been inserted up to 12 mm into the plasma of ohmically heated discharges with low/medium plasma current, $I_p = 0.6 \div 1.0$ MA, and low/medium density $n_e = 0.5 \div 3 \cdot 10^{19}$ m^{-3} ($n/n_G = 0.05 \div 0.4$). In order to assure a proper limiter operation, most of the discharges have been executed with the feedback controlled *q(a)* set to zero. In some discharges, *q(a)* has been set to -0.025, well above the threshold.

3. Heat flux and decay length computation

Fig. 3 shows two examples of temperature measurement performed on two q(a)≈0, 0.6/1.0 MA, medium/low density pulses. Differently from similar measurements performed on tokamak devices [9], RFX-mod shows a 2D distribution of the surface temperature, with large asymmetries both in poloidal and in toroidal directions. This makes the commonly used 2D (1D on surface/1D in depth) THEODORE [10,11] or quadrupoles [12] codes unsuitable

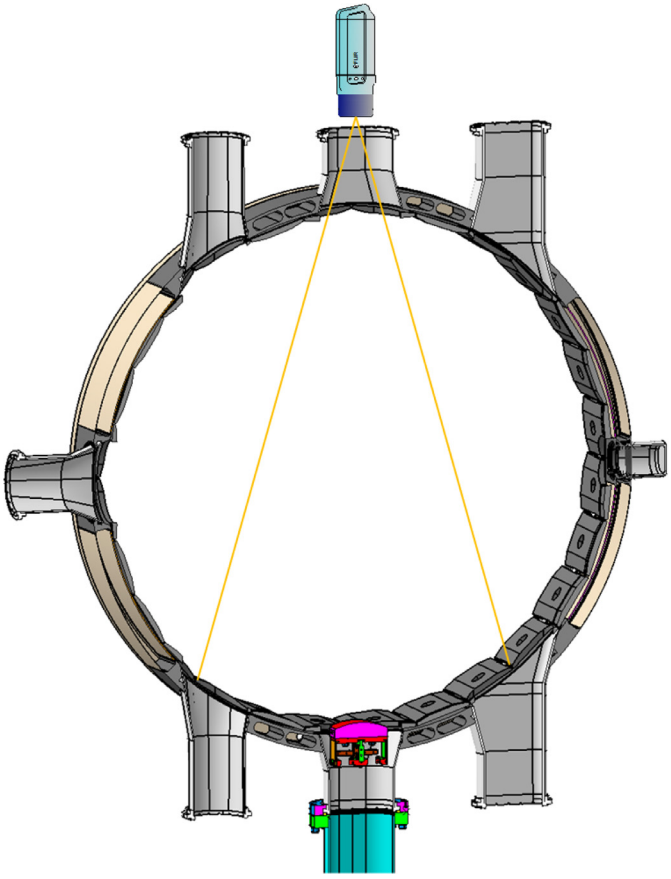

Fig. 2. Layout of the limiter (at bottom), infrared camera (at top) and vacuum vessel.

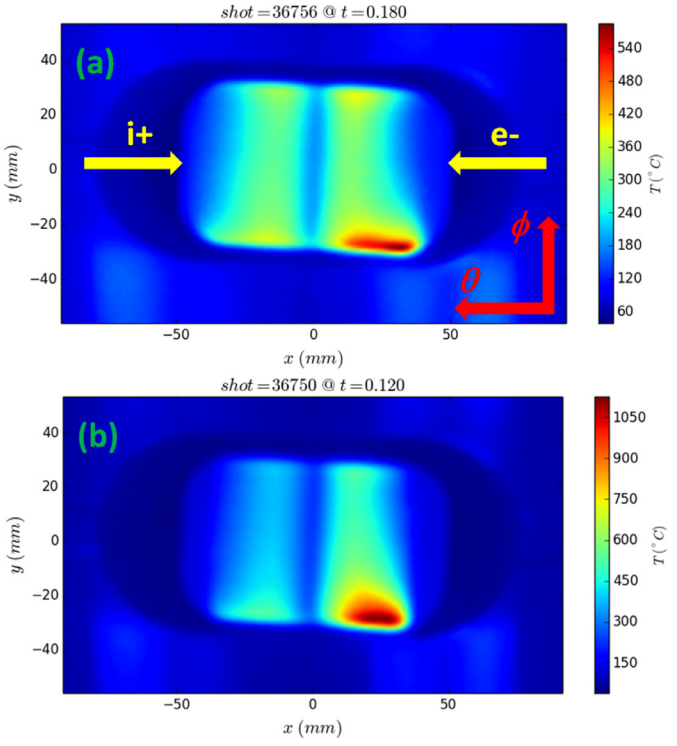

Fig. 3. Two examples of infrared temperature measurement: (a) 0.6 MA medium density, q(a)= 0 pulse; (b) 1.0 MA low density, q(a)= 0 pulse.

Please cite this article as: P. Innocente et al., Heat flux measurements and modelling in the RFX-mod experiment, Nuclear Materials and Energy (2017), http://dx.doi.org/10.1016/j.nme.2017.01.020

to compute heat flux from temperature. For this reason the heat flux has been computed solving and inverting the heat conduction problem with a novel 3D code named TtoP3D. The code integrates the 3D heat equation:

$$\rho C_p \frac{\partial T}{\partial t} - \frac{\partial}{\partial x}\left(k_x \frac{\partial T}{\partial x}\right) - \frac{\partial}{\partial y}\left(k_y \frac{\partial T}{\partial y}\right) - \frac{\partial}{\partial z}\left(k_z \frac{\partial T}{\partial z}\right) = \dot{q}_v$$

where $\vec{k} \equiv (k_x(T), k_y(T), k_z(T))$ is the thermal conductivity, which can depend on temperature and direction, ρ is the material density, C_p is the specific heat and $\dot{q}_v$ is the volumetric heat generation. The equation is integrated on a 3D rectangular mesh with a variable mesh size to account non-parallelepiped limiters and high temperature gradients at the interacting surface, the volumetric heat generation is set equal to the impinging plasma heat flux on the surface facing the plasma where the temperature is measured and zero elsewhere. At each time the heat flux is evaluated iteratively: at the zero order approximation it is computed using the analytical solution of the 1D heat diffusion equation, higher order approximations are computed by numerically integrating heat equation and adding (or subtracting) the heat flux (evaluated as for the zero-order) coming from the difference between the computed temperature and the measured one. The iterations are repeated till the maximum temperature difference between the computed and the measured is less than a reference measurement error (1 °C in our case). It is found that about 3÷5 iterations are enough to reach the desired precision. Differently from the analysis of previous IR measurements performed on tokamak tiles the effect of a surface layer [10,12,13] has not been included in the following analysis because the short exposure time of samples to the plasma prevents the formation of a significant layer of carbon coating or dust deposition. The results of the code have been compared with those of the THEODORE code for a 1D (on surface) case and the two gave results in agreement. For one experimental case the TtoP3D computed heat flux has been used in an ANSYS model of the limiter, to compute the surface temperature obtaining a good agreement with the measured one. An example of the computed heat flux for an RFX-mod pulse is shown in Fig. 4.

One simple parameter that characterizes the edge transport is the decay length of the plasma parallel heat flux. We can compute it after converting the heat flux perpendicular to the limiter surface (P_S) to those parallel (P_D) and perpendicular ($P_\perp$) to the magnetic surfaces. In the general case the heat flux on surface is related to the plasma heat fluxes by the relation: $P_S = \sin\alpha P_\parallel + \cos\alpha P_\perp$ where α is the angle between the magnetic surface and the limiter surface. The evaluation of the parallel heat flux is simple if the contribution of the perpendicular one is negligible, but this is not our case: Fig. 4b shows that the heat flux computed at the top the cylindrical limiter (where the parallel contribution is null) has a minimum, but the value is not negligible with respect to what computed elsewhere. For this reason we have assumed a constant relation between the parallel and perpendicular heat fluxes ($f = P_\perp/P_\parallel$) and fitted the heat flux on the limiter using the relation:

$$P_S(x) = P_{0\parallel}[\sin\alpha(x) + f\cos\alpha(x)]e^{-\frac{\Delta(x)}{\lambda}}$$

where x is the coordinate in the poloidal direction and Δ is the distance from the top of the limiter in the radial direction, while P_{0D}, f and λ are the free fitting parameters, the last one in particular is the heat flux decay length. Heat fluxes have been fitted separately on the ion and electron drift sides. Fig. 4b shows an example of two fits displaying a good match between measured and fitted data; some disagreement appears at the edges but those points correspond to $\Delta \approx 6$ mm which is more than two times the decay length.

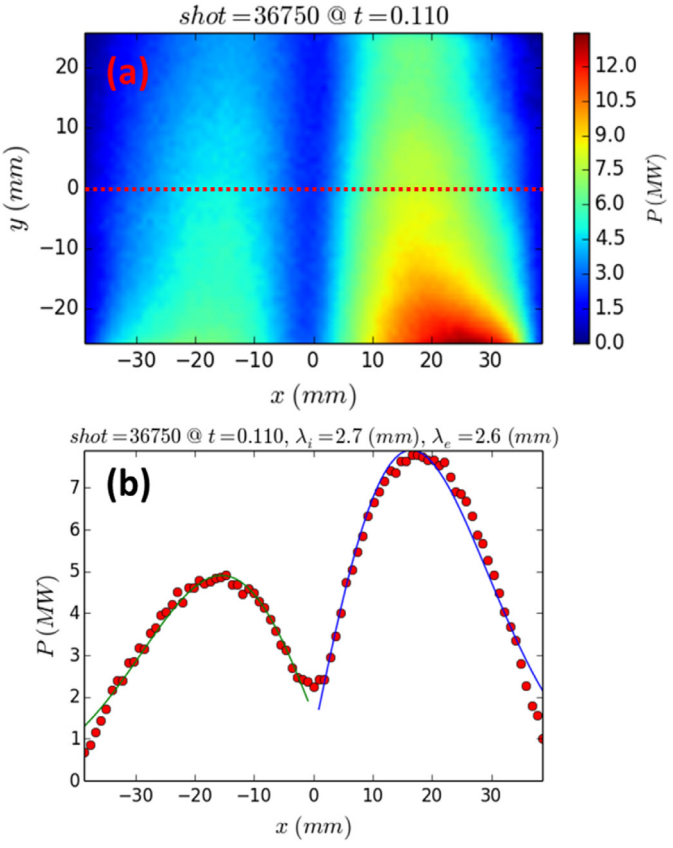

Fig. 4. Heat flux computation and fitted profile: a) heat flux on limiter surface, b) heat flux profile along the dashed line in frame a), red dots are computed values, green and blue lines fit profiles on the ions and electrons drift sides. (For interpretation of the references to colour in this figure legend, the reader is referred to the web version of this article.)

4. Results

As stated in the introduction, one element that makes difficult the study of the edge in the RFX-mod device is the deformation of the LCFS. This deformation strongly affects also the present analysis because the position of the limiter with respect to the plasma changes in time depending on the local shift and the plasma minor radius. For this reason to correctly analyse heat fluxes it is necessary to evaluate the local position of the limiter with respect to the local LCFS. In RFX-mod the distortion of the plasma boundary can be computed from external measurements using the linearized, incompressible ideal-MHD Faraday–Ohm's Law [14]. The LCFS is then defined as the first flux surface touching the graphite wall when the boundary deformation is added to the toroidally symmetric horizontal plasma shift (which is usually negligible in RFX-mod). Fig. 5a shows the relative distance between the LCFS and the top of the limiter for a limiter insertion of 10 mm; it is possible to see that, due to the time variation of the boundary deformation, the relative position varies between -10 mm (when the maximum of the deformation is close to the limiter) and about + 10 mm. In the same figure the red and green lines highlight the correlation between the plasma-limiter distance and the average heat flux on the limiter (panel b): when the distance is at maximum the heat flux is minimum (green lines), on the contrary minimum distances correspond to maximum of heat flux (red lines). The same plot shows that the correspondence does not always hold, for example at about 0.1 s the high heat flux on the limiter does not correspond to a minimum of the distance. A more detailed analysis of this case shows that it corresponds to a situation in which the maximum of

Please cite this article as: P. Innocente et al., Heat flux measurements and modelling in the RFX-mod experiment, Nuclear Materials and Energy (2017), http://dx.doi.org/10.1016/j.nme.2017.01.020

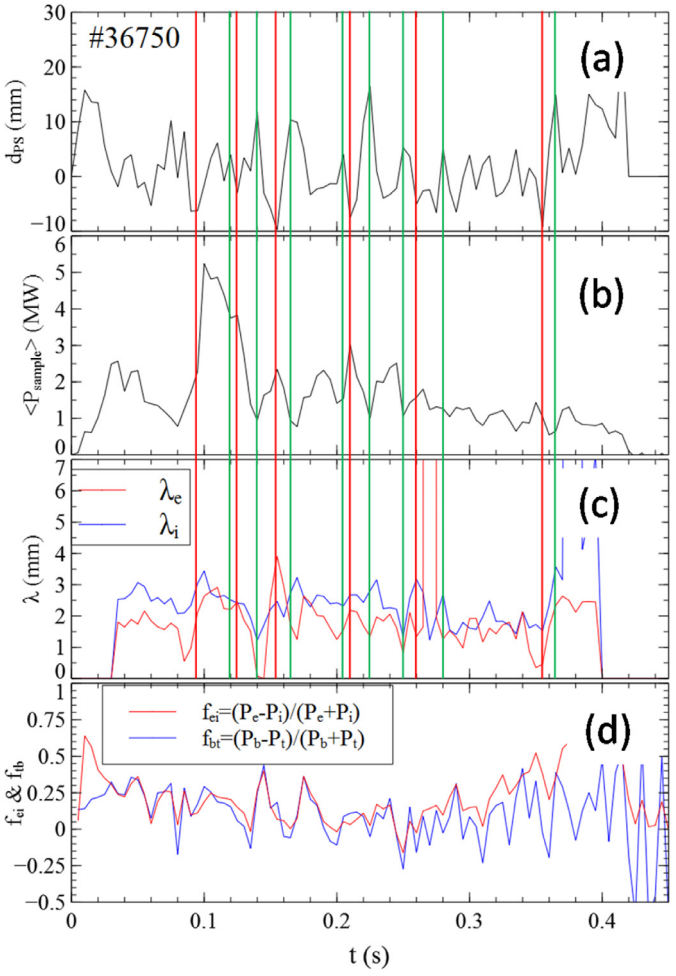

Fig. 5. a) Distance between LCFS and limiter, b) average heat flux on limiter, c) electron and ion decay lengths, d) heat flux ratio between two half sides of the limiter: ion and electron, bottom and top sides.

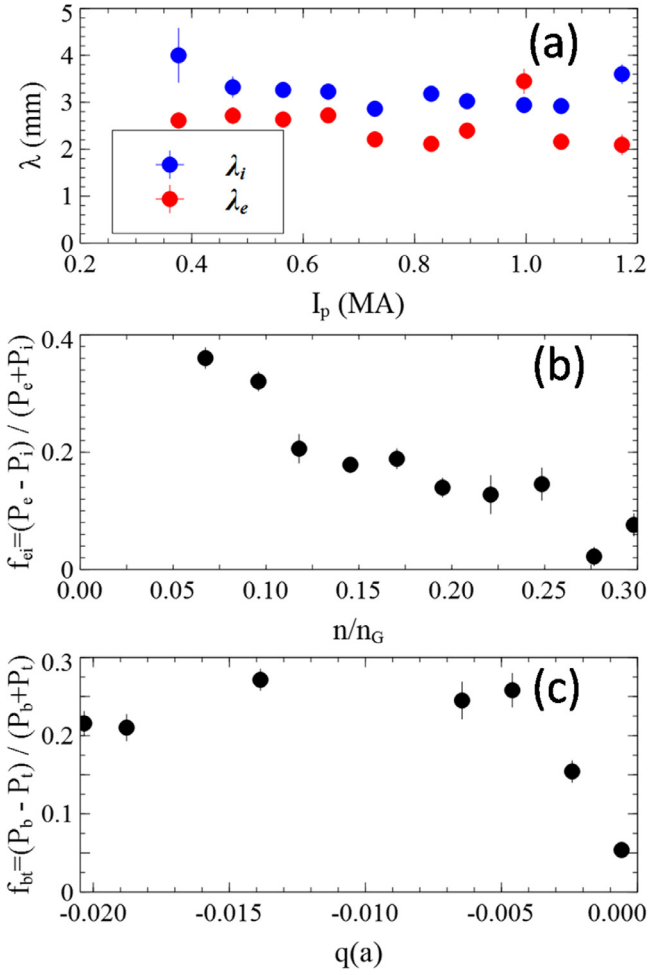

Fig. 6. a) Ion and electron decay lengths versus plasma current; b) $(P_e-P_i)/(P_e+P_i)$ ratio versus n/n_G; c) $(P_b-P_t)/(P_b+P_t)$ bottom/top asymmetry in function of the safety factor.

the deformation is very close to the limiter, a situation where additional effects (not only the distance from the LCFS) can play a role in PWI.

In Fig. 5c the ion and electron decay lengths are drawn: λ_i is typically 3 mm and always higher than λ_e by about 0.5–1.0 mm. Sometimes the decay lengths (in particular λ_e) assume low values, these correspond to the times in which plasma-limiter distance is high and the limiter is exploring the very far part of the SOL tail. In the same discharge the $f = P_\perp/P_\parallel$ factor (not plotted in the figure) assume values 0.05/0.02 in the ion/electron drift sides. These values are in agreement with those that can be derived from the "funnelling" model developed by P.C. Stangeby et al. [15] $P_\perp/P_\parallel = (2D_\perp/L_f c_s)$ with $D_\perp \approx 1\,m^2/s$ and L_f half of the length of the limiter.

In order to characterize the heat flux poloidal and toroidal asymmetries we have divided the surface of the limiter in four regions: the half left (ion) and right (electron) parts and the half bottom and top parts. We have then computed the power asymmetry factors $f_{ei}=(P_e-P_i)/(P_e+P_i)$ and $f_{bt}=(P_b-P_t)/(P_b+P_t)$ which are shown in Fig. 5c and d. In this low density discharge $f_{ei}\approx 0.25$ (lower values are usually associated to higher plasma density) showing an higher heat flux on the electron drift side; at high plasma current some correlation between f_{ei} and the appearance of the QSH states has been also observed, with lower f_{ei} values in presence of the QSH. The f_{bt} shows a strong correlation with f_{ei}, with positive values associated to electron side dominated heat fluxes.

To get a better insight on the average behaviour of the heat flux at the edge, the parameters previously introduced for a single discharge have been averaged on many discharges and analysed in terms of controllable plasma parameters (Fig. 6). Only data times in which the plasma-limiter distance was less than ±5 mm have been used. No clear dependence on the plasma parameters has been found for the heat flux decay lengths; as seen in the single pulse of Fig. 5: λ_i is usually longer than λ_e by about 0.5 mm (Fig. 6a), with some indication (but inside the error bars) that they decrease with plasma current and with density (not shown in the picture). It is interesting to note that these decay lengths are similar to those obtained in big size tokamaks like ASDEX and JET [16]. Furthermore the weak dependence of the decay lengths on density and current (which in RFX-mod is approximately proportional to P_{SOL} since P_{SOL}z P_{OHM}zV·I and Vzconst) recalls the similar result found with the "two-point" models for the power e-folding distance [17] in the low density sheath-limited regime of the diverted tokamaks.

The f_{ei} ratio (Fig. 6b) shows a more clear dependence on n/n_G, it reaches values up to about 0.4 at the lowest n/n_G and then it decreases reaching values close to zero when $n/n_G > 0.25$. The e/i asymmetry was already measured with calorimetric and Langmuir probes [1] and its origin cannot be associated to the externally applied local electric field because at q(a)≈0 the external electric field is perpendicular to the field line direction. For this reason in previous RFP works the parallel heat flux asymmetry and the superthermal electron population measured at the edge [18] were

Please cite this article as: P. Innocente et al., Heat flux measurements and modelling in the RFX-mod experiment, Nuclear Materials and Energy (2017), http://dx.doi.org/10.1016/j.nme.2017.01.020

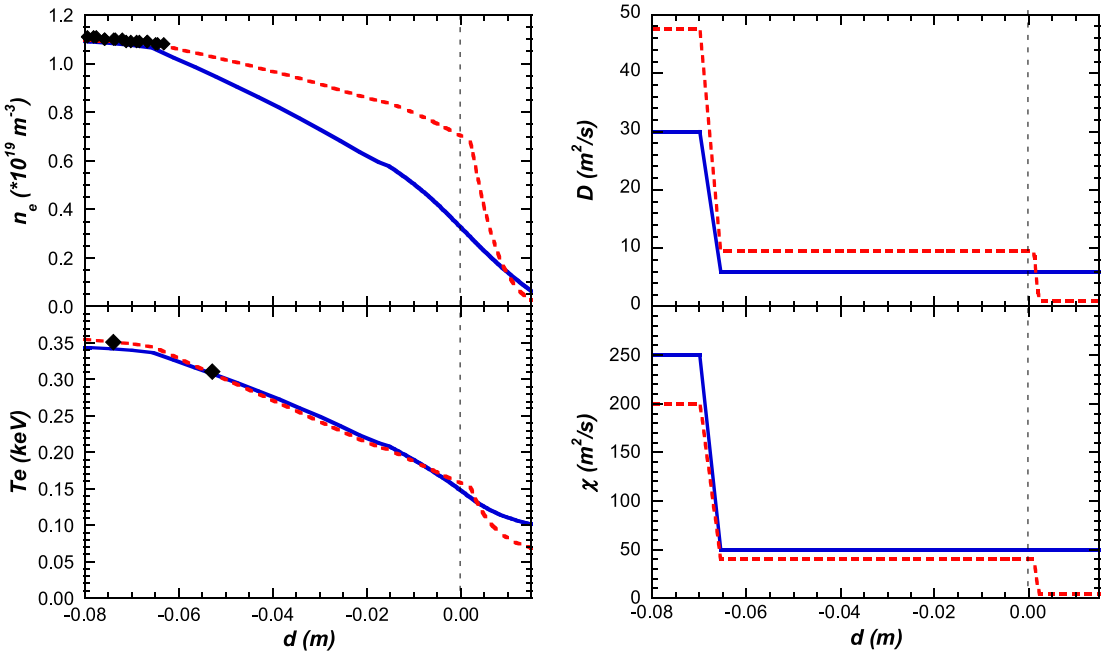

Fig. 7. Edge/SOL density (n_e) and temperature (T_e) at the equatorial plane computed with SOLEDGE2D-EIRENE for a low density 700 kA pulse and two transport profiles (D, χ). Diamonds show experimental values measured with interferometer and Thomson scattering, the vertical dash line represents the position of LCFS.

considered a proof of the KDT theory [19], which describes the sustainment of the RFP magnetic configuration as the results of the diffusion toward the edge of the high energy electrons generated in the plasma core by the toroidal electric field. The validity of the KDT theory against the dynamo MHD theory, which predicts the production by the magnetic fluctuations of an electric field parallel to the magnetic one, was questioned later [20] but the source of superthermal electron population measured at the edge it is still more easily associated to the diffusion from the core of high energetic electrons. The present result, which shows a strong reduction of the heat flux asymmetry with increasing density, can be explained on the basis of the KDT as a result of the reduction of the electron collisional mean free path (λ_0). This does not mean that the core generated electrons are the source of the whole poloidal current at the edge (as it is in the KDT theory) but that at low density they can significantly contribute to it. Finally the f_{bt} ratio (Fig. 6c) shows a constant value for negative q(a) and approach a null value at q(a)=0 suggesting that the field line angle is the source of the heat flux asymmetry: when the field lines are exactly perpendicular to the limiter the asymmetry disappear.

5. Edge modelling

To get some insight into the plasma transport properties of the edge and of the SOL, the code SOLEDGE2D-EIRENE has been used [2]. It is a 2D transport code with a multi-species plasma solver coupled to EIRENE for neutrals; it solves the continuity equations for densities, parallel velocities, temperatures and electric potential. One of the main advantages of SOLEDGE2D code is the ability to simulate the plasma up to the first wall (FW) [2]. In other codes, e.g., UEDGE [21] and EDGE2D [22] the computational domain usually does not extend up to the FW or, like for the SOLPS code, custom solutions are adopted to deal with the FW [23,24]. Instead in SOLEDGE2D the FW is managed by the penalization method [25,26], which extends the solution of fluid equations inside the wall and controls the sharp gradients which form at the wall interface by the penalization parameter. The method enables the modelling of very complex FW geometry by simply adjusting the penalization mask that splits the solid and plasma regions. This is a major requirement in the RFX-mod case considering the absence of a limiter able to keep plasma far from the FW and the shaped surface of the FW tiles (see Fig. 2).

To evaluate transport parameters (D and χ) in the edge and SOL plasma regions, they have been optimized to match measured density, temperature, particles influxes and heat flux decay length on the limiter with those computed by the simulations. As regards temperature and density, the comparison is limited to nearly-edge plasma region because in RFX-mod SOL profile measurements are not routinely available at high plasma current. In the experiments described in this paper, electron temperature was measured with the core multipoint Thomson scattering (TS) system which provides reliable measurements up to about 5 cm from the wall [27]. Electron density was computed by Abel inverting the integral of the line density measured with a 8 chord mid-infrared CO_2 interferometer [28]; based on the maximum impact parameter of interferometer chords (h_{max}=0.33/0.46) and density profile shape the computed density can be considered meaningful up to about 5–6 cm far from the wall. Averaged particle influx has been evaluated from H_α measurements available at several poloidal and toroidal locations. For simplicity the flat slopped limiter has been simulated. In setting up SOLEDGE2D-EIRENE simulation many simplifying assumptions have been done: the localized limiter and the magnetic equilibrium have been considered toroidally symmetric, using the magnetic equilibrium measured at the toroidal position of the limiter; the ohmic input power has been attributed 50–70% to electrons and 50–30% to deuterium ions, in RFP devices this is a strong assumption because there are many uncertainties about the mechanism of ion heating through collisions with electrons or anomalous heating (see ref. [29] and there in); thermal conductivity has been assumed equal between electrons and ions ($\chi_e L \chi_i$) which is also a strong assumption considering the uncertainties in the nature of the transport at the edge/SOL. Due to the previously described limitation in terms of available measurements and of modelling assumptions, the final aim of the comparison was not to get exact values and profiles for the transport parameters but

Please cite this article as: P. Innocente et al., Heat flux measurements and modelling in the RFX-mod experiment, Nuclear Materials and Energy (2017), http://dx.doi.org/10.1016/j.nme.2017.01.020

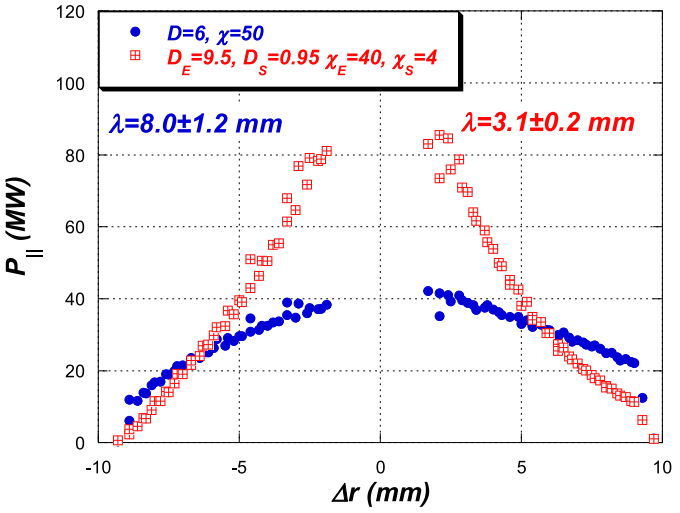

Fig. 8. Plot of the parallel heat flux profiles computed at the limiter with constant transport parameters (blue closed circles) and lowered SOL transport parameters (red open squares). (For interpretation of the references to colour in this figure legend, the reader is referred to the web version of this article.)

to provide an approximated indication of their values and their radial behaviour. Several set of transport parameters (D and χ) have been tested. The simplest schematization assumed the same value of D and χ in the plasma edge and SOL (flat profile across the last closed flux surface) and for discharges at 700 kA a good matching of temperature, density and influxes was obtained with D = 3–6 m^2/s and χ = 20–60 m^2/s. These values are in good agreement with previous evaluations of D and χ_e at plasma edge performed with the ASTRA code from profiles measurements in RFX-mod [30,31], but they did not provide the heat flux profiles measured on the limiter. Instead, in order to match also the heat flux profiles, it is necessary to assume D and χ reduced by a factor of about ten in the SOL with respect to plasma edge. Fig. 7 shows the results of two SOLEDGE2D-EIRENE simulations of a low density 700 kA discharge with the two transport coefficient profiles: constant in the edge/SOL regions (blue) and with ten times reduction of D and χ in the SOL (red). In both simulations 60% of the 12 MW input power was assigned to electron (40% to ions) and transport parameters were changed to match the measured density, temperature and average particle influx. For the same simulations, Fig. 8 shows (with the same colour code) the parallel heat flux profiles on the limiter and the computed decay lengths. In Fig. 8 it is clearly seen that the high transport values in the SOL produce a large spread of the heat flux which is not in agreement with our experimental evaluation of the decay length (Fig. 6a), instead the ten times reduced transport values are able to reproduce the measurements.

A possible explanation of the lower values of the transport parameters in the SOL is based on the RFX-mod experimental observation that the edge transport is mainly due to poloidal blobs (or long filaments) of increased pressures moving radially [32]: in our case the presence of the limiter reduces blobs transport cutting their length and radial size.

6. Conclusions

In RFX-mod for the first time the edge transport has been analysed and modelled by means of thermography measurements and edge fluid code.

The measurements confirmed the presence of increased heat flux in the direction of the electron drift side at low density. This result is in agreement with previous RFP findings, the novelty of this measurement is the identification of the density threshold above which the asymmetry disappears. The agreement of such threshold with that observed for the achievement of Quasi Singles Helicity states in RFX-mod [5] could be a coincidence but could also be the indication that, as described in the KDT theory, at low density a fraction of the poloidal current is due to superthermal electrons, reducing the demand on the MHD dynamo.

The modelling performed with the SOLEDGE2D-EIRENE code has shown that the transport is drastically reduced in the SOL region compared to the edge one. This has been ascribed to a reduction of filaments dimension which decreases the turbulent transport. The resulting very short heat flux decay length has important consequences on the PWI, increasing the peak power on edges of wall tiles as it has been observed in RFX-mod [33].

References

[1] V. Antoni, et al., J. Nucl. Mater 220-222 (1995) 650.
[2] H. Bufferand, et al., J. Nucl. Mater. 438 (2013) S445.
[3] P. Sonato, et al., Fus. Eng. Des. 161 (2003) 66.
[4] P. Martini, et al., Nucl. Fus. 53 (2015) 104018.
[5] R. Lorenzini, et al., Nat. Phys. 5 (2009) 570.
[6] M.E. Puiatti, et al., Nucl. Fus. 55 (2015) 104012.
[7] FLIR A655sc Infrared Camera, http://www.flir.com/science/display/?id=46802.
[8] E. Delchambre-Demoncheaux, et al., J. Nucl. Mater. 415 (2011) S1178.
[9] T. Eich, B. Sieglin, A. Scarabosio, W. Fundamenski, R.J. Goldston, A. Herrmann ASDEX Upgrade Team, Phys. Rev. Lett 107 (2011) 215001.
[10] A. Herrmann, ECA 25A (2001) 2109.
[11] A. Herrmann, et al., Plasma Phys. Control. Fus. 37 (1995) 17.
[12] J.-L. Gardarein, et al., Int. J. Therm. Sci. 48 (2009) 1.
[13] P. Andrew, et al., J. Nucl. Mater. 313–316 (2003) 135.
[14] P. Zanca, D. Terranova, Plasma Phys. Control. Fus. 46 (2004) 1115.
[15] P.C. Stangeby, C.S. Pitcher, J.D. Edler, Nucl. Fus. 32 (1992) 2079.
[16] R. Mitteau, et al., J. Nucl. Mater. 313–316 (2003) 1229.
[17] C.S. Pitcher, P.C. Stangeby, Plasma Phys. Control. Fus. 39 (1997) 779.
[18] J.C. Ingraham, R.F. Ellis, J.N. Downing, C.P. Munson, P.G. Weber, G.A. Wurden, Phys. Fluids B 2 (1990) 143.
[19] A.R. Jacobson, R.W. Moses, Phys. Rev. A 29 (1984) 3335.
[20] L. Garzotti, B. Pégourié, R. Bartiromo, P. Innocente, S. Martini, Phys. Rev. Lett. 84 (2000) 5532.
[21] M.E. Rensink, et al., J. Nucl. Mater. 266–269 (1999) 1180.
[22] R. Simonini, et al., Contrib. Plasma Phys. 34 (1994) 368.
[23] F. Subba, et al., Comp. Phys. Comm. 179 (2008) 194.
[24] M. Baelmans, et al., Nucl. Fus. 51 (2011) 083023.
[25] L. Isoardi, et al., J. Comp. Phys. 229 (2010) 2220.
[26] A. Paredes, et al., J. Nucl. Mater. 438 (2013) S625.
[27] A. Alfier, R. Pasqualotto, Rev. Sci. Instrum. 78 (2007) 025005.
[28] P. Innocente, S. Martini, Rev. Sci. Instrum. 63 (1992) 4996.
[29] R.M. Magee, et al., Phys. Rev. Lett. 107 (2011) 065005.
[30] R. Lorenzini, et al., Nucl. Fus. 52 (2012) 062004.
[31] F. Auriemma, Nucl. Fus. 55 (2015) 043010.
[32] P. Scarin, M. Agostini, R. Cavazzana, F. Sattin, G. Serianni, M. Spolaore, N. Vianello, J. Nucl. Mater. 390–391 (2009) 444.
[33] A. Canton, et al., Characterization of first wall materials in RFX-mod, in: 43rd European Physical Society Conference on Plasma Physics, Leuven, Belgium, 2016.

Please cite this article as: P. Innocente et al., Heat flux measurements and modelling in the RFX-mod experiment, Nuclear Materials and Energy (2017), http://dx.doi.org/10.1016/j.nme.2017.01.020